Journal of
NANOSTRUCTURES
JNS
NANOSTRUCTURES
JNS.kashanu.ac.ir

Sol-Gel Synthesis, Characterization and Optical Properties of Bi^{3+}-Doped CdO Sub-Micron Size Materials

Abdolali Alemi[a], Shahin Khademinia[a*], Sang Woo Joo[b], Mahboubeh Dolatyari [c], Hossein Moradi [d]

[a]*Department of Inorganic Chemistry, Faculty of Chemistry, University of Tabriz, Tabriz, Iran*

[b]*School of Mechanical Engineerng WCU nano research center,Yeungnam University,Gyongsan 712-749 , South KOREA*

[c]*Laboratory of Nano Photonics & Nano Crystals, School of Engineering-Emerging Technologies, University of Tabriz, Tabriz, Iran*

[d]*Faculty of chemistry, Islamic Azad University, Ardabil Branch, Ardabil, Iran*

Article history:
Received 11/1/2013
Accepted 4/5/2013
Published online 1/6/2013

Keywords:
Sol-Gel Method
Cadmium Oxide
Bismuth
Optical Properties
PXRD

**Corresponding author:*
E-mail address:
shahinkhademinia@gmail.com
Phone: +98 9116224110
Fax: +98 1326373157

Abstract

Highly crystalline Bi^{3+}-doped cadmium oxide (CdO) sub-micron structures were synthesized by calcination the obtained precursor from a sol-gel reaction. The reaction was carried out with cadmium nitrate ($Cd(NO_3)_2.4H_2O$), bismuth nitrate ($Bi(NO_3)_3.5H_2O$) and ethylene glycol ($C_2H_6O_2$) reactants without any additives at 80°C for 2h. Resulting gel was calcined at 900 °C with increasing temperature rate of 15°C per minute for 12 h in a furnace. As a result of heating, the organic section of gel was removed and Bi^{3+}-doped cadmium oxide micro structure was produced. The obtained compound from the sol-gel technique possesses a cubic crystalline structure at micro scale. Powder x-ray diffraction (PXRD) study indicated that the obtained Bi^{3+}-doped CdO has a cubic phase. Also, SEM images showed that the resulting material is composed of particles with the average diameter of 1 μm. Also, UV–vis and FT-IR spectroscopies were employed to characterize the Bi^{3+}-doped CdO micro structures.

1. Introduction

Over the last decades, Bi_2O_3-based materials with high oxygen ionic conductivity have been extensively studied for their potential use as solid electrolyte in fuel cell [1], high purity oxygen generators and electrochemical sensors [2]. Also bismuth oxide is an important metal-oxide semiconductor [3]. Owing to these peculiar characteristics, Bi_2O_3 has been studied in various fields and is widely used in electrolyte, electro reduction, and sensor optical coatings as well as in transparent and superconductor ceramic glass

manufacturing [4]. For these reasons we chose Bi_2O_3 as dopant material. Also, the films of transparent conductive oxides (TCO) such as zinc oxide and cadmium oxide (CdO) have been extensively studied because of their use in semiconductor optoelectronic device technology [5]. CdO films have been successfully used for many applications, including use in gas sensor devices, photo diodes, transparent electrodes, photo transistors, and photovoltaic solar cells [6]. Also, CdO is an n-type semiconductor with a cubic crystal structure, possesses a direct band gap of 2.2 eV [7]. Beside, CdO shows very high electrical conductivity even without doping due to the existence of shallow donors caused by intrinsic interstitial cadmium atoms and oxygen vacancies [8]. In previous works, synthesis of Sn-doped CdO thin films [9], Bi^{3+}-doped CdO thin films by sol–gel spin coating method with different raw materials and heat treatment that resulted different morphology[10], copper doped CdO nanostructures [11], ZnO doped CdO materials [12], titanium-doped CdO thin films [14], ZnO–CdO–TeO_2 system doped with the $Tb^{3+}$and Yb^{3+} ions [15], N-doped CdO [16], samarium, cerium, europium, iron and lithium-doped CdO nanocrystalline materials [13, 17, 18, 19, 21], indium doped CdO films [20], gallium doped CdO thin films [22], Gd doped CdO thin films [23], Li–Ni co-doped CdO thin films [24], aluminum-doped CdO [25, 26], fluorine-doped CdO Films [27], La doped CdO[28], Dy doped CdO films[29], carbon doped CdO[30], Mn Doped Nanostructured CdO[31], boron dope CdO [32] have been performed.

In this work, crystalline Bi^{3+} doped CdO sub-micron size structures have been synthesized by sol-gel method, with cadmium nitrate, bismuth nitrate ($Bi(NO_3)_3.5H_2O$) and ethylene glycol ($C_2H_6O_2$) as raw materials without using any catalyst or template at a heat treatment temperature of 900°C with increasing temperature rate of 15°C per minute for 12h reaction time, which is a very simple and economical method. Also, we discussed about dopant concentration effect on the morphology of the synthesized materials. The product was characterized by PXRD, SEM, FT-IR and UV-vis techniques.

2. Materials and Methods

All chemicals were of analytical grade, obtained from commercial sources and used without further purification. Phase identifications were performed on a powder X-Ray diffractometer Siemens D5000 using Cu K_α radiation (λ=1.542Å). The morphology of the obtained materials was examined with a Philips XL30 Scanning Electron Microscope (SEM). Absorption spectra were recorded on a Jena Analytik Specord 40. Also FT-IR spectra were recorded on a Tensor 27 Bruker made in Germany.

2.1 Synthesis of $Bi_xCd_{1-x}O$ micro-size layer (x = 2, 3 and 3.2%)

4.78 mmolar (1.958 mmol), 4.73 mmolar (1.94 mmol) and 4.72 mmolar (1.935 mmol) (Mw=308.482 $g.mole^{-1}$) cadmium nitrate ($Cd(NO_3)_2.4H_2O$), 0.098 mmolar (0.04 mmol), 0.146 mmolar (0.06 mmol) and 0.156 mmolar (0.064 mmol) (Mw=485.071 $g.mole^{-1}$) bismuth nitrate ($Bi(NO_3)_3.5H_2O$), respectively and 10 ml ethylene glycol ($C_2H_6O_2$) were added in 400 ml distilled water. Then, the solution was stirred at 80 °C for 2h until a dried gel was obtained. The gel was brown color and spongy. The dried obtained gel was treated thermally at 900 °C for 12 h. After the reaction completed, and cooled slowly to room temperature, the obtained material was pulverized. The sample was black like powder.

3. Results and discussion

3.1 PXRD analysis

In order to investigate the structural properties of Bi^{3+} - doped CdO micro structures X-ray diffraction measurement varying the diffraction angle, 2, from 4◦ to 70◦ were performed. Powder X-ray diffraction (PXRD) patterns of CdO micro structures calcinated at 900 ◦C in air are shown in Fig. 1. The diffraction peaks at 2θ values of 33.10°, 38.32°, 55.32°, 65.96° and 69.31° matching with the 111, 200, 220, 311, and 222 of cubic CdO (JCPDS-05-0640) indicated the formation of CdO with excellent crystallinity. Fig. 1 represents the XRD patterns of the obtained materials after 12 h thermally reaction time at 900°C at x_{Bi}=2, 3 and 3.2 mmole, respectively. Fig. 1(d) shows that with increasing the dopant amount to x_{Bi3+}=3.2 mmol, some peaks arises in about 2ϴ≈37, 56° that assigned to Bi_2O_3 [33-38]. So the doping limitation is x=0-3 mmole. The inter planar spacing (d) was calculated via Bragg's law ($n\lambda = 2d_{hkl} \sin\theta$)) where n is called the order of reflection (we used n=1), d is interplanar spacing, ϴ is the half of diffraction angle and λ is the incident X-rays of wavelength. Because the radii of Bi^{3+} (r=0.96Å [1]) is smaller than the radii of Cd^{2+} (r=1.55 Å), compared to PXRD patterns of the pure CdO, the diffraction lines in the PXRD patterns of Bi^{3+}- doped CdO shift to higher 2ϴ. So (*Δ2θ=33.10 (doped) - 32.97 (pure) =0.13),* (Δd=2.7135 (pure) - 2.703 (doped)=0.0105Å). Because Bi_2O_3 (fcc crystal phase) and CdO have cubic crystal structure, and so they are iso-crystal phase, when Bi is coming into CdO unit cell in the place of Cd, because the radius of Bi is smaller than Cd, so there is a contraction in the CdO unit cell. So we conclude that as a result of the contraction in the obtained crystal the inter planar space will be reduced. Also, with using celref software version 3, the cell parameter for highest amount of Bi doped CdO is as follow: 4.6912 Å while for pure CdO, the cell parameter is 4.6950. So the pure CdO and Bi doped CdO cell volume are 103.4920 and 103.2409, respectively. Also, Crystal sizes of the obtained materials were measured via Debye Scherer's equation $t = \frac{0.9\lambda}{B_{\frac{1}{2}} \cos\theta_B}$, where ***t*** is entire thickness of the crystalline sample, $B_{1/2}$ of FWHM is the full width at half its maximum intensity and Θ_B is the half diffraction angle at which the peak location is, that are as follows: 28.2, 26.3, 25.4, 23.4 nm for pure CdO, and 2, 3 and 3.2 dopant concentration mmole. The pattern shows polycrystalline structure of cubic CdO structure (NaCl structure of a space group Fm3m). The lattice constant calculated for an undoped CdO sample, was **a**=0.46950 nm (JCPDS 05-0640). The PXRD measurements confirm that a pure phase of the cubic CdO is formed [39-45].

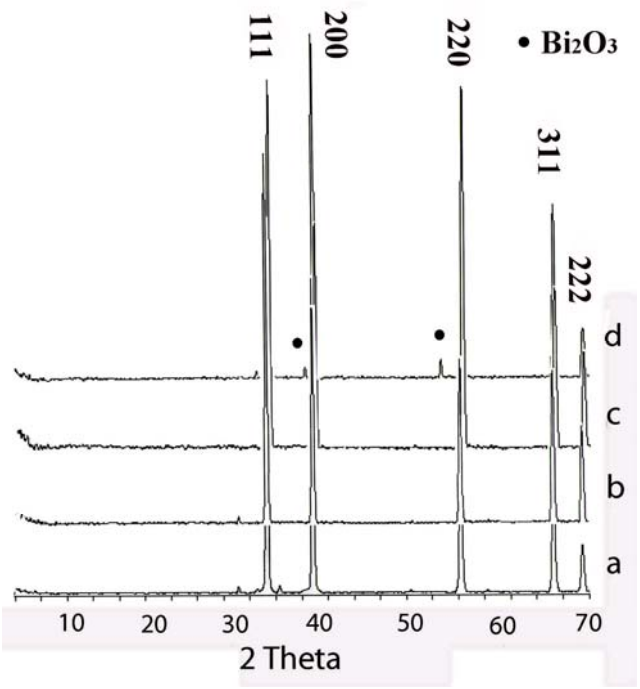

Fig. 1. PXRD patterns of the synthesized $Cd_{1-x}Bi_xO$ micro size materials, where (a) is pure CdO, (b) x = 2; (c) is x = 3; and (d) is x = 3.2 mole%.

3.2 Microstructure analysis

Fig. 2 reveals the SEM images of cubic structure of obtained crystalline CdO at 900 °C [45]. Remarkably, it was observed that the average particle size is at the range of 2 µm. As shown in fig. 2(a) and (b), it's clear that the material is composed of particles with heterogeneous size. Fig. 2(c) shows that the sample is composed of multigonal particles with heterogeneous size. Fig. 2(d) and (e) show that the morphology is clearly layered like, as a resulted of calcination treatment, with the particle almost spherical shape and the width size in a range of about 1 to 3 µm.

The SEM images of the synthesized Bi^{3+}-doped CdO micro-size materials are given in Fig. 3 and 4. Fig. 3 shows SEM images of $Cd_{0.98}Bi_{0.02}O$ micro-size particle. The average width size of the spherical shaped particles that formed layer structures is in a range between 1 to 2 µm. Since the images for the pure and doped materials are not similar we concluded the dopant concentration at which the material was obtained has influence on the particle morphology. Fig. 3(a) and (b) show that there are cavities in the form of macro-porous that caused from thermally treatment at calcinations in 900°C. Fig. 3(c) and (d) show that due to doping Bi^{3+}, there are more cavities as porosity in the obtained material. In this figure it is clear that the particle sizes are heterogeneous. Also, it's clear that there are particles on the surface of the material that the size of them is about 500 nm to 1 µm. Fig. 3(e) and (f) show high magnification of the cross section of each particle and it seems that they are composed of compact layers. Fig. 4 shows SEM images of $Cd_{0.97}Bi_{0.03}O$ micro-size particle. Fig. 4(a) and (b) show both macro-porous structure and the cavity in the particle composed the layered like material. In Fig. 4(c) and (d) it seems that there are small particles as uncus on the surface of each particle. With higher magnification in fig. 4(d), it is clear that the cavity size is about 500 nm. With low magnification in fig. 4e and (f), it seems that with increasing the dopant amount to 3 mole%, the morphology of the particles are changed to particles with regular shape and edge, but the size of the particles is still heterogeneous and the macro-porosity in the structure is clear.

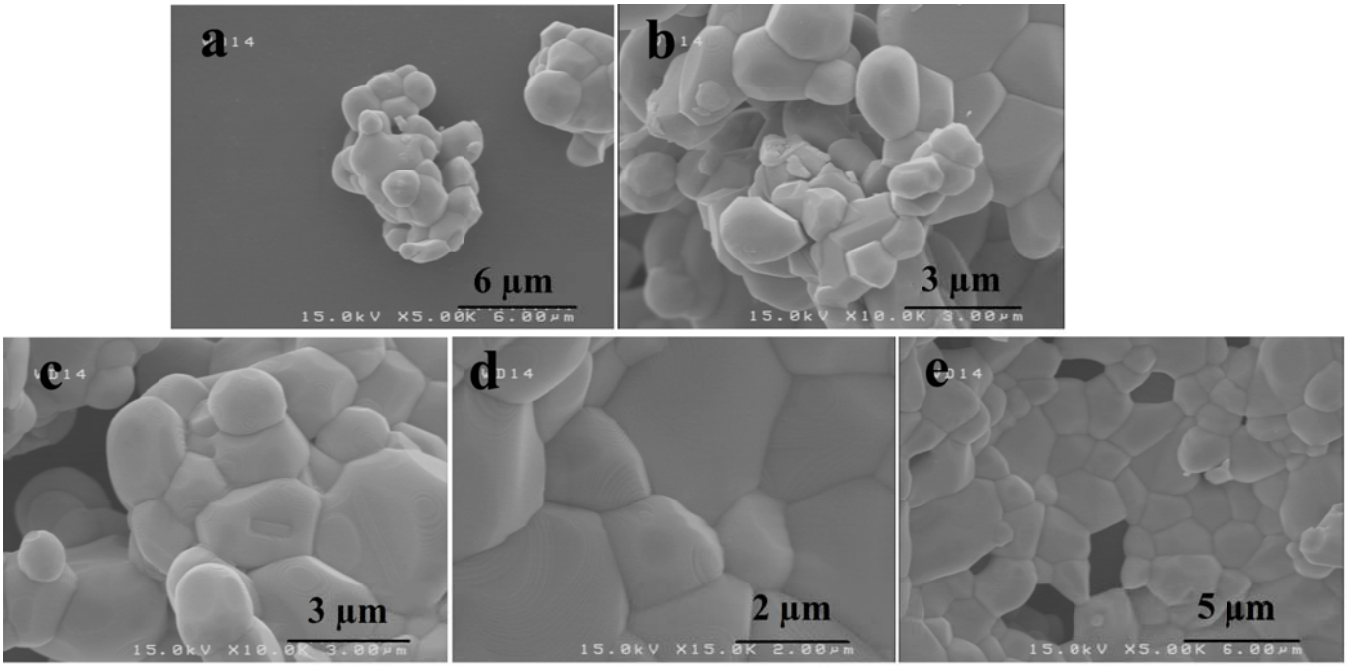

Fig. 2. The SEM images of the synthesized pure CdO micro size materials.

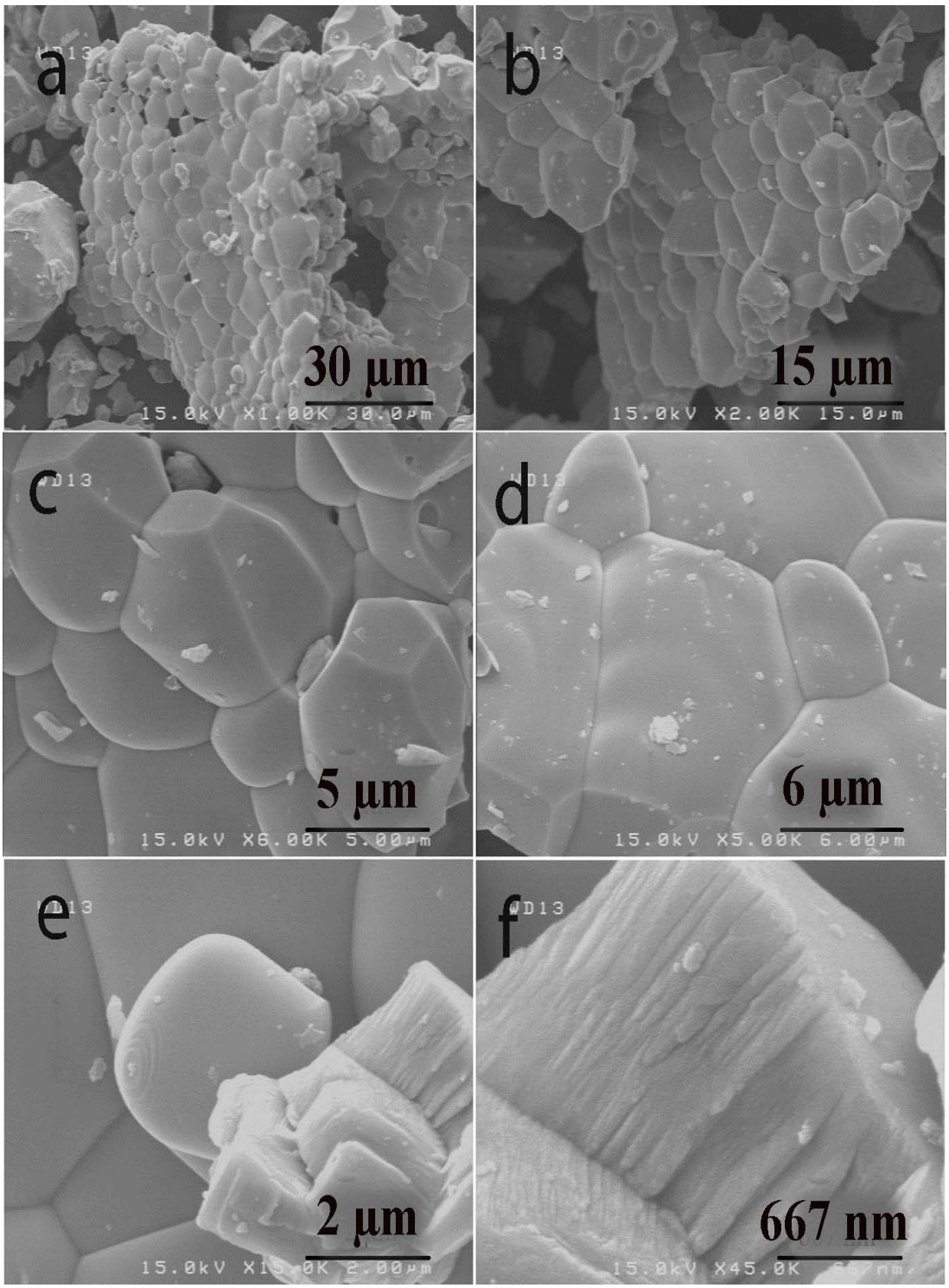

Fig. 3. The SEM images of the synthesized $Cd_{0.98}Bi_{0.02}O$ micro size materials.

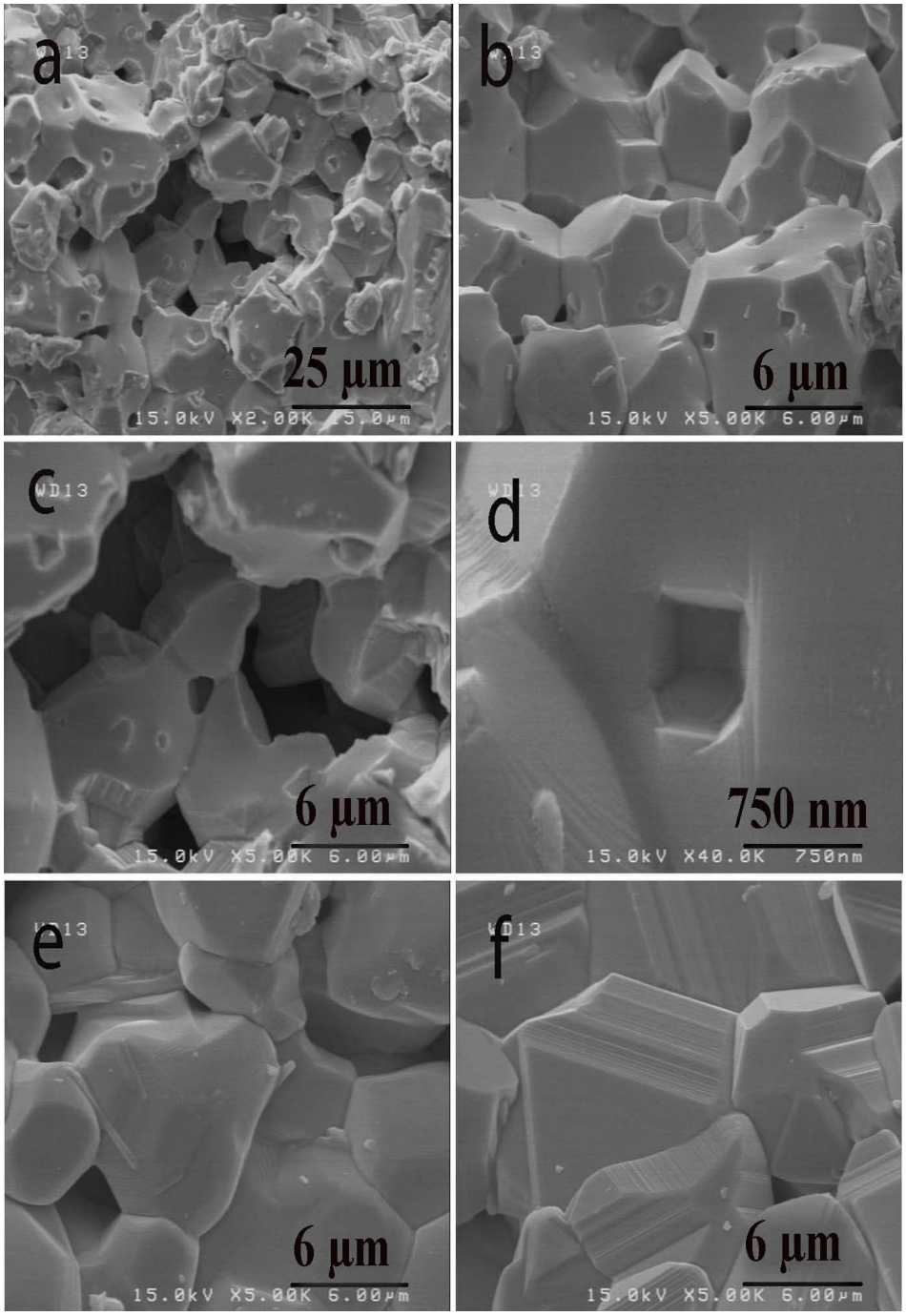

Fig. 4. The SEM images of the synthesized $Cd_{0.97}Bi_{0.03}O$ micro size materials.

3.3 Spectroscopic studies

Fig. 5 shows the electronic absorption spectra of the synthesized Bi^{3+} -doped CdO micro-size materials. According to the spectra, Bi_2O_3 presents the photoabsorption properties from UV light region to visible light, shorter than 470 nm, which is assigned to the intrinsic band gap absorption. So in fig. 4a in x_{Bi3+} = 2 mole%, there is a broad band in about 370 nm that is behind the CdO band and a weak peak in around 1050 nm that corresponded to CdO [39, 46, 47]. With increasing the dopant amount to 3 mmole, there is a

broad band in a range of about 420 nm (E_{gap} = 2.95 eV), partially behind the CdO band that is corresponded to Bi^{3+} [3, 34, 35].

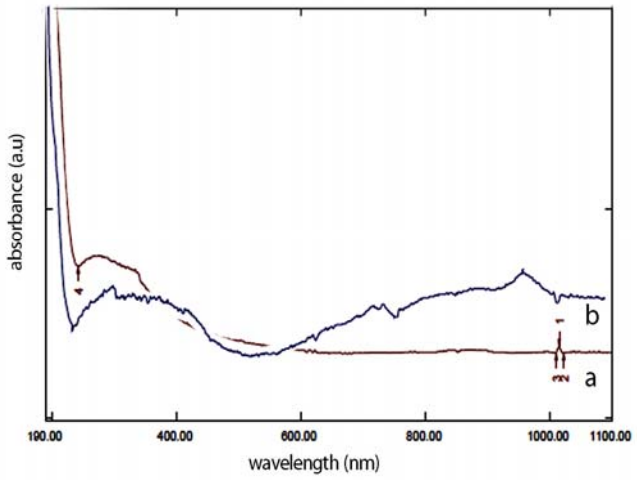

Fig. 5. The electronic absorption spectra of the synthesized $Cd_{1-x}Bi_xO$ micro size materials, where (a) is x = 2 and (b) is x = 3 mole%.

Fig. 6 shows FT-IR spectrum diagram of the doped samples. From the present spectrum, it is clear that the peak at 3443 cm^{-1} is corresponded to stretching vibration of H_2O molecule [48]. Peak at 1457 cm^{-1} is corresponded to carbonate and peaks at 470 and 543 cm^{-1} are corresponded to CdO [48]. Also we know that the peaks at 800 to 1400 cm^{-1} are assigned to CdO [49]. Peak at 1560 cm^{-1} can be assigned to a residual organic component [45]. The intensive signal around 850 cm^{-1} appeared in FTIR spectra of both 6(a) and (b) are the stretching vibration of Bi–O bonds in BiO_6 octahedra which suggests the stability of nanocrystalline Bi_2O_3 during the photocatalytic reaction [34]. Additionally, several new peaks from 400 to 600 cm^{-1} attributed to vibration of Bi–O bonds of BiO_6 octahedra [36]. The additional peak at 595 cm^{-1} is reported to be the vibration of Bi–O bonds of BiO_6 coordination polyhedra in α-Bi_2O_3 [36]. Beside, an absorption band at about 1060 cm^{-1} is also observed that may be attributed to the other kinds of vibrations of Bi–O caused by the interaction between the Bi–O bonds and their other surroundings [36].

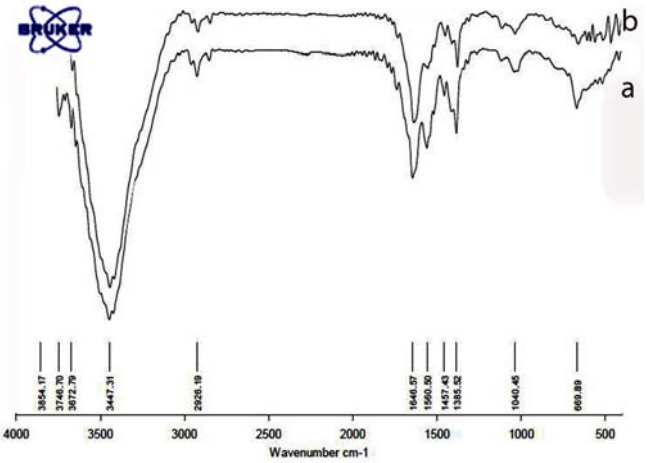

Fig. 6. FT-IR spectrum of the synthesized $Cd_{1-x}Bi_xO$ micro-size materials, where (a) is x = 2 and (b) is x = 3 mole%.

4. Conclusion

In summary, micro-layers of Bi^{3+}-doped CdO were synthesized successfully by employing a simple sol-gel method. We found that the dopant concentration affects the morphology of the final product. As shown by SEM images, with increasing the dopant concentration, the morphology of the layered like material was changed. We found that compared to those of the micro-size material of pure CdO, the diffraction lines in the powder XRD patterns of Bi^{3+}-doped CdO shift to higher 2θ values. The shift in the diffraction lines might be attributed to the smaller radius of the dopant ion, compared to the ionic radius of the Cd^{2+}, which may cause a contraction of the unit cell and so decrease lattice parameters in the Bi^{3+}-doped CdO materials. The synthesized materials exhibited electronic absorption optical properties in the UV-visible region, which show dependence on the dopant amounts in the structure. These materials are expected to have a potential application in semiconductor devices, as catalysts, etc.

Aknowledgement

The authors expresses their sincere thank to the authorities of University of Tabriz for financing the project.

References

[1] L. Ying, w. Changzhen, J. rare earths. 26 (2008) 337-340.

[2] Zhen. Qiang, M. Girish, le. Ka, Shi. Gang, Li. Rong, He. Weiming, Liu. Jianqiang, Sol. State Ion. 176 (2005) 2727-2733.

[3] Xie. Jimin, Lu. Xiaomeng, Chen. Min, Zhao. Ganqing, Song. Yuanzhi, Lu. Shuaishuai, Dyes and Pig. 77 (2008) 43-47.

[4] Wu. Xiaohong, Qin. Wei, L. Li, Guo. Yun, Xie. Zhaoyang, Catal. Com. 10 (2009) 600-604.

[5] CH. Champness, CH. Chan, Sol. Energy Mater. Sol. Cells. 37 (1995) 72-75.

[6] X. Liu, Z. Xu, Y. Shen, Lisbon. (1997) 585-587.

[7] M. Ortega, G. Santana, A. Morales-Acevedo, Solid State Electron. 44 (2000) 1765-1769.

[8] R. Haul, D. Just, J. Appl. Phys. 33 (1962) 487-493.

[9] B.J. Zheng, J.S. Lian, L. Zhao, Q. Jiang, Optical and electrical properties of Sn-doped CdO thin films obtained by pulse laser deposition. Appl Surf Sci 85 (2011) 861-865.

[10] F. Dagdelen, Z. Serbetci, R.K. Gupta, F. Yakuphanoglu, Mater. Lett. 80 (2012) 127-130.

[11] M. Benhaliliba, C.E. Benouis, A. Tiburcio-Silver, F. Yakuphanoglu, A. Avila-Garcı´a, A. Tavira, R.R. Trujillo, Z. Mouffak, J. Lumin. 132 (2012) 2653-2656.

[12] NeseKavasoglu, A. Sertap Kavasoglu, Sener Oktik, J. Phys. Chem. Sol. 70 (2009) 521-525.

[13] A.A. Dakhel, Thin Solid Films. 518 (2010) 1712-1715.

[14] R.K. Gupta, K. Ghosh, R. Patel, P.K. Kahol, Appl. Surface Science. 255 (2008) 2414-2418.

[15] C. Ruvalcaba-Cornejo, M. Flores-Acosta, Ma. Elena Zayas, R. Lozada-Morales, J. Lumin. 128 (2008) 213-214.

[16] Varghese. Neenu, L.S. Panchakarla, M. Hanapi, A. Govindaraj, C.N.R. Rao, Mater. Research Bul. 42 (2007) 2117-2120.

[17] A.A. Dakhel, Solid State Sciences. 13 (2011) 1000-1005.

[18] A.A. Dakhel, Mater. Chem. Phys. 117 (2009) 284-287.

[19] A.A. Dakhel, Mater. Chem. Phys. 130 (2011) 398-402.

[20] Kose. Salih, Atay. Ferhunde, Bilgin. Vildan, Akyuz. Idris, Inter. J. hydrogen energy. 34 (2009) 5260-5266.

[21] A.A. Dakhel, Optical Mater. 31 (2009) 691-695.

[22] Kul. Metin, Zor. Muhsin, Aybek. Ahmet Senol, Irmak. Sinan, Evren Turan, Sol. Energy Mater. Sol. Cells. 91 (2007) 882-885.

[23] R.J. Deokate, S.V. Salunkhe, G.L. Agawane, B.S. Pawar, S.M. Pawar, J. Alloys and Comp. 496 (2010) 357-363.

[24] R.K. Gupta, K. Ghosh, R. Patel, P.K. Kahol, J. Alloys and Comp. 509 (2011) 4146-4149.

[25] R.K. Gupta, Z. Serbetc, F. Yakuphanoglu, J. Alloys and Comp. 515 (2012) 96-99.

[26]N. Ozdemir, M. Cavas, Ahmed A. Al-Ghamdi, Zarah H.Gafer, F. El-Tantawy and F. Yakuphanoglu. Proceedings of Global Engineering, Science and Technology Conference. 1 - 2 April, Dubai, UAE, ISBN: 978-1-922069-21-4 (2013).

[27] R. Maity, K.K. Chattopadhyay, Sol. Energy Mater. Sol. Cells. 90 (2006) 597-606.

[28]Z.A. Alahmed, Z. Serbetçi and F. Yakuphanoglu. Acta physica polonica A. 124 (2013).

[29]A. A. Dakhel. Eur. Phys. J. Appl. Phys. 45, (2009) 20303.

[30]Quan Gu, Huaqiang Zhuang, Jinlin Long, Xiaohan An, Huan Lin, Huaxiang Lin, and Xuxu

Wang. International Journal of Photoenergy. 2012 (2012), Article ID 857345, 7 pages.

[31]S. Amutha, R. Chandiramouli and B.G. Jeyaprakash. Journal of Applied Sciences, 12, (2013) 1641-1645.

[32]F. Yakuphanoglu. Solar Energy - solar energ. 85, (2011) 2704-2709.

[33] A.A. Dakhel, J. Alloys and Comp. 475 (2009) 51-54.

[34] Zhang. Lisha, Wang. Wenzhong, Yang. Jiong, Chen. Zhigang, Applied Catalysis A: General. 308 (2006) 105-110.

[35] Prasad Manjusri. Sirimanne, Takahashi. Kazunori, Sonoyama. Noriyuki, Sakata. Tadayoshi, Sol. Energy Mater. Sol. Cells. 73 (2002) 175-187.

[36] Wang. Changhua, Shao. Changlu, Wang. Lianjia, Zhang. Lina, Li. Xinghua, Liu. Yichun, J. Colloid and Interface Science. 333 (2009) 242-248.

[37] D. Ling. Christopher, J. Solid State Chem. 177 (2004) 1838-1846.

[38] Woo. Kim. Hyoun, Thin Solid Films. 516 (2008) 3665-3668.

[39] H.B. Lu, L. Liao, H. Li, Y. Tian, D.F. Wang, J.C. Li, Q. Fu, B.P. Zhu, Y. Wu, Mater. Lett. 62 (2008) 3928-3930.

[40] Aksoy. Seval, Caglar. Yasemin, Ilican. Saliha, Caglar. Mujdat, Inter. J. hydrogen energy. 34 (2009) 5191-5195.

[41] O. Vigil, F. Cruz, A. Morales-Acevedo, G. Contreras-Puente, L. Vaillant, G. antana, Chem. and Phys. 68 (2001) 249-252.

[42] A.A. Dakhel, Thin Solid Films. 517 (2008) 886-890.

[43] R.R. Salunkhe, V.R. Shinde, C.D. Lokhande, Sensors and Actuators: B. 133 (2008) 296-301.

[44] Fahrettin. Yakuphanoglu, Mujdat. Caglar, Yasemin. Caglar, Saliha. Ilican, J. Alloys and Comp. 506 (2010) 188-193.

[45] A. Alemi, S. W. Joo, S. Khademinia, M. Dolatyari, A.Bakhtiari, h.moradi. submitted manuscript. International nano letters. (2013).

[46] T.P. Gujar, V.R. Shinde, Kim. Woo.Young. Jung, C.D. Kwang. Deog, Oh. Shim. Joo, Lokhande, Applied Surface Science. 254 (2008) 3813-3818.

[47] S. Ashoka., P. Chithaiah., G.T. Chandrappa, Mater. Letters. 64 (2010) 173-176.

[48] M. Ristic, S. Popovic, S. Music, Mater. Letters. 58 (2004) 2494-2499.

[49] A. Tadjarodi, M. Imani, Mater. Letters. 65 (2011) 1025-1027.